J. Mat. NanoSci. 2016, 3(1), 33-40 Article

Journal of
Materials NanoScience

Characterization and evaluation of biological and photocatalytic activities of selenium nanoparticles synthesized using yeast fermented broth

K. Gnaneshwar Goud[1], Naveen Kumar Veldurthi[2], M Vithal[2], Gopal Reddy[1]*

[1]Department of Microbiology, [2]Department of Chemistry, University College of Science, Osmania University, Hyderabad-500 007. India

Received on: 18-Nov-2016, Accepted and Published on: 20-Dec-2016

ABSTRACT

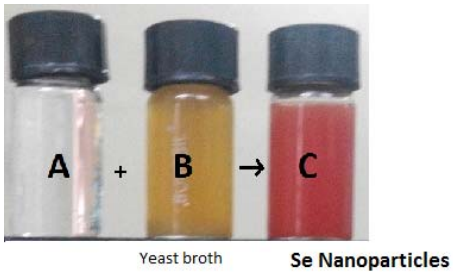

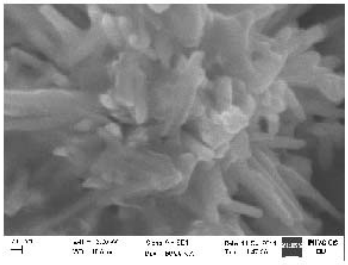

The present article reports an environmentally benign and unexploited method of green synthesis of selenium nanoparticles (SeNPs) using an agro-waste based yeast fermented broth as a reducing agent. Treatment of aqueous solution of Na_2SeO_4 with agro-waste based yeast fermented broth yielded stable selenium nanoparticles. The UV-Visible spectroscopy of nanoparticle solution showed absorption maxima at 540nm. SEM observations revealed the predominance of 170–240nm rod shaped particles arranged as "flower-like" crystalline aggregates. SeNPs showed potent antibacterial activity against common biofilm-forming Gram-positive bacteria *Staphylococcus aureus* and significant anti-proliferative activity against A549, MCF7, and SKOV3 (cancer) cell lines. The SeNPs exhibited a concentration dependent increase in antioxidant activity. Further, the green-synthesized SeNPs have also been tested as photocatalyts for degradation of methylene blue (model dye), under visible light illumination at room temperature and the rate of degradation has been studied spectrophotometrically.

Keywords: Selenium nanoparticles, Yeast fermented broth, antibacterial, anti-proliferative, antioxidant, Photocatalytic degradation

INTRODUCTION

Nanotechnology is a rapidly growing interdisciplinary study that covers many areas of science, research and technology. The overwhelming demand for NPs in various applications has led to the outcome of novel synthetic strategies including chemical, physical and biological methods. However chemical and physical techniques face drawbacks of high production cost and are often found to involve the use of harsh chemicals which are potentially dangerous for the environment and have several occupational exposure hazards.[1-4] A quest for an environmentally sustainable synthetic process has provoked to search for a safe bioreduction process yielding nanoparticles. The use of biological materials like microorganisms or their products and plant extracts for synthesis of nanoparticles is regarded as simple, mild and environmental friendly.[2,5-8] Among the different types of nanoparticles, Selenium has received substantial interest due to its low toxicity, higher bioavailability, and good absorption capacity which attribute multidisciplinary applications in medical diagnostics and nano-biotechnology.

*Corresponding Author: Prof. Gopal Reddy
Department of Microbiology, University College of Science,
Osmania University, Hyderabad-500 007. India
Email: gopalred@hotmail.com

Cite as: *J. Mat. NanoSci. 2016, 3(2), 33-40.*

 ISSN 2394-0867 http://pubs.iscience.in/jmns

Dyes are a group of synthetic organic compounds that are used as colorants in leather, textile, paper, food, plastic, cosmetic, and pharmaceutical industries[9]. Industrial effluents containing dyes is forming a serious environmental threat, as disposal of these effluents into natural water bodies often leads to environmental contamination, serving as a source of non-aesthetic pollution, eutrophication and thereby affecting the aquatic life.[10,11] The removal or degradation of recalcitrant synthetic dyes is a crucial ecological problem and pose a challenge. Different methods like electrolysis, oxidation, coagulation, membrane filtration, ozonization, active sludge biochemical processes, bio-degradation etc. have been commonly used for the removal / elimination of synthetic dyes from waste water.[12-15] These established technologies are often found unable to curtail the contaminant concentration adequately to a desired level with efficacy. Since the synthetic dyes have complex chemical structures, they are highly rebellious to reduction or degradation by sunlight, physico-chemical treatments and microbial biodegradation.[16] Also these systems suffer from incomplete removal and the formation of byproducts that are even more toxic than the starting materials. In this context, need arises for the development of improved and better waste water treatment processes.

The advent of nanoparticles as catalysts in various chemical processes present a solution for safe, simple, eco-friendly degradation of organic dyes.[17] During recent times, degradation of dyes by semiconductor based photocatalysts using solar energy has received more attention.[18-20] Inorganic semiconductors are generally used as photocatalysts, with titanium dioxide, having become the most widely investigated.[21-24] However its utility is restricted, as it is non-responsive in visible light range ($\lambda > 400$ nm),[25] which contributes around 46% of the total solar energy, and a search for alternate photocatalysts functional in visible range would be necessary. Selenium, an important semiconductor metal and is well exploited for its photovoltaic and optoelectronic properties.[26] According to literature, not much has been reported about the green-synthesis of SeNPs and its application as photocatalyst. Methylene blue, a cationic thiazine dye (Color Index Number: 52015), which is generally used in a wide range of fields, such as medicine, biology and chemistry is preferred as a model compound, in the present work for evaluation of photocatalytic activity of SeNPs. Though methylene blue is not vigorously hazardous, however, acute exposure can cause detrimental effects like tissue necrosis, vomiting, cyanosis, Heinz body formation, shock, quadriplegia, and increased heart rate in humans.[27,28]

The present study aims at green synthesis of selenium nanoparticles, their characterization and evaluation of antibacterial, anticancer, antioxidant and photocatalytic activities.

MATERIALS AND METHODS

Sodium selenite, methylene blue, peptone, yeast extract and malt extract were purchased from Himedia, Mumbai, sucrose from S.D. fine chemicals and n-Hexanol from Qualigens. All glassware was thoroughly cleaned before the experiments. Deionized water (DI) was used in the preparation of all solutions.

Biosynthesis and purification of selenium nanoparticles:

The green synthesis of SeNPs was performed by mixing 1mL of an agro waste based yeast fermented broth[29] with 10mL of 2mM sodium selenite and incubated at room temperature for 24h. The mixtures were observed for color change and an increase in absorbance. Selenium nanoparticles formation Appearance of red color in the reaction mixture is indicated. At different time intervals, a small volume (1mL) of samples were drawn and their absorbance was measured by UV-Visible spectrophotometry.

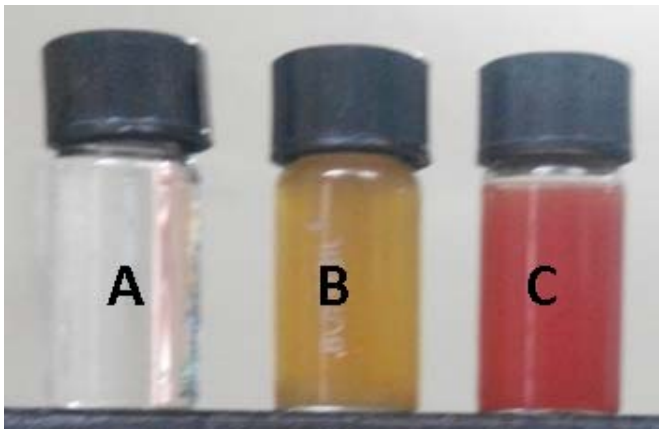

Figure 1 Green synthesis of SeNPs using an agrowaste based yeast fermented broth (a) 2mM Sodium selenite solution (b) Fermented broth (c) Reaction mixture at 12h.

The SeNPs were extracted from the reaction mixture by aqueous-two-phase extraction system using n-hexanol as described by Sonkusre et al., 2014, where the SeNPs get dispersed in aqueous phase and the protein and other contaminants in organic phase.[35] The top organic phase along with proteins and other contaminants is discarded and the NPs were harvested by high speed centrifugation at 12000 rpm for 30 minutes. To the pellet, 5 mL of distilled water and 5mL n-hexanol were added and mixed vigorously for few minutes and left undisturbed. On standing, the SeNPs get settled at the bottom of aqueous phase, which are washed with distilled water and lyophilized for further studies.

Characterization

UV-Visible spectral analysis

The ultra violet-visible spectroscopy has been proved to be a very convenient, efficient and quite sensitive tool for preliminary conformation of nanoparticles synthesis due to the intense absorption peak exhibited by the formed nanoparticles. The reduction of pure Se ions was monitored by measuring the UV-vis spectrum (Hitachi U-2910 Spectrophotometer, Japan) of the reaction mixture at different time intervals. UV-Visble spectroscopic analysis was performed by continuous wavelength scanning from 200 nm to 800 nm and 2 mM sodium selenite solution was used for the baseline correction.

SEM and EDX analysis

The morphology and size of the purified SeNPs were studied with a scanning electron microscope (JEOL-JSM 6390, Japan). Energy dispersive spectroscopy (EDX) analysis was conducted with the same instrument to confirm the elemental composition of the sample.

X-ray diffraction analysis

The crystallographic structure of purified SeNPs was examined by Philips Panlytical X'pert Pro X-ray diffractometer system operated at a voltage of 40kv and current of 30mA with cu kα radiation in θ - 2θ configurations. The diffracted intensities were recorded from 10° to 80° 0f 2θ angles.

Differential scanning calorimetry

Thermogravimetric differential scanning colorimeter (TG-DSC) analysis of the synthesized NPs was carried out using TG–DSC (SDT Q600 model, TA Instruments, USA). About 5 mg of the sample was taken in an alumina cup holder and heated up to 1000 ^{0}C at the rate of 10 ^{0}C/min.

Antibacterial activity of selenium nanoparticles

The bacterial pathogens *Staphylococcus aureus, Escherichia coli, Bacillus subtilis* and *Pseudomonas aeruginosa* were obtained from the MTCC. The strains were maintained on nutrient agar slants at 4°C. The minimum inhibitory concentration (MIC) was determined according to the standard broth micro-dilution method. SeNPs were dissolved in sterile nutrient broth, serially diluted to obtain different concentrations and inoculated with the test organisms (10^5–10^6 CFU/ml). Nutrient broth without addition of SeNPs and sodium selenite salt, inoculated with test organism served as control.

Anticancer activity of selenium nanoparticles

MCF7, A549 and SKOV3 (cancerous cell lines) and CHO (normal cell lines) were obtained from National Center for Cell Sciences (NCCS), Pune, India. The cells were maintained in Dulbecco's modified eagle medium (DMEM) with l-glutamine and 4.5 g/L glucose, 10% fetal bovine serum (FBS), penicillin G (100 units/mL) and streptomycin sulfate (0.1 mg/mL) at 5% CO_2 and 37 °C. Cytotoxic effect of SeNPs in MCF7, A549, SKOV3 and CHO cells was examined by 3-(4,5-dimethylthiazol-2-yl)-2,5-diphenyltetrazolium bromide (MTT) assay. Approximately, 1×10^4 (cells/well) cells seeded in 96 well plates were treated with different concentrations of SeNPs and incubated for 24 h. Following incubation, 20 µL of MTT (5 mg/mL) was added to cells and incubated for 4 h. The purple colored formazan crystals formed were dissolved in 100 µL of dimethyl sulfoxide (DMSO) and the absorbance was measured at 570 nm with reference 630 nm. All experiments were performed twice in triplicates and the average of all the experiments was recorded as cell-viability percentage in comparison with the control experiment, while SeNP untreated controls were considered as 100% viable. The percentage inhibition of cells was calculated by using the formula:

Inhibition % = ((Absorbance $_{control}$ − Absorbance $_{Test}$) / Absorbance $_{control}$) x 100

Antioxidant activity of selenium nanoparticles

DPPH free radical scavenging assay

DPPH free radical scavenging activity (DRSA) of SeNPs was determined according to the method of Shimada et al., (1992) with minor modifications.[30] One mL of DPPH solution (500 µM) in methanol, was added to 1 mL of SeNP solution. Distilled water was used as control. The mixture was vortexed, allowed to stand in dark at ambient temperature for 30 min, and absorbance was measured at 517nm. Ascorbic acid (500 µg/mL) was used as positive control. The lower absorbance of the reaction mixture indicated a higher percentage of scavenging activity. The percentage of inhibition or scavenging of free radicals was determined by the following formula:

DRSA (%) = (($A_{control}$ –A_{sample}) / $A_{control}$) x 100

Where, $A_{control}$ is the absorbance of control and A_{sample} is the absorbance of the sample

Reducing power assay

The Fe^{+3} reducing antioxidant power was measured using the method developed by Zhang et al., (2008) with minor modifications[31]. To 1mL of SeNP solution, 2.5 mL of 0.2 M phosphate buffer (pH 6.6) and 2.5 mL of 1% potassium ferricyanide were added, vortexed properly and incubated at 50 °C for 20 min. After cooling to room temperature, 2.5 mL of 10% trichloro-acetic acid was added to the reaction mixture and centrifuged. Then, 2.5 mL of supernatant was mixed with 2.5 mL of distilled water and 1 mL of 0.1% ferric chloride. After a 10-min reaction time, the absorbance of the resulting solution was measured at 700 nm. Increase in absorbance of the reaction mixture indicates high reducing power of the sample.

Total antioxidant capacity

Total antioxidant capacity was evaluated with the assay based on the reduction of Mo (VI) to Mo (V) by the SeNP solution and subsequent formation of a green phosphate / Mo (V) complex at acidic pH.[32] A 1 mL aliquot of SeNP solution was mixed with 1 mL of reagent solution (0.6 M sulfuric acid, 28 mM sodium phosphate, and 4 mM ammonium molybdate), incubated at 95 °C for 90 min, then the mixture was allowed to cool to room temperature, and the absorbance was measured at 695 nm against a blank. Higher the absorbance, greater is the antioxidant capacity of a sample.

Photocatalytic activity:

Photocatalytic degradation of methylene blue

The photocatalytic activity of SeNPs was investigated through the evaluation of photodegradation of methylene blue (model compound) under visible light. For this, a visible annular type photoreactor (Heber Scientific, India, model HVAR1234) with 300W tungsten lamp positioned inside a cylindrical quartz vessel and surrounded by a water circulating cooling jacket was used. To a 50 mL of methylene blue solution (10mg/L), 50 mg of SeNps was added and air was bubbled to effectively stir the solution and to keep the suspended catalyst particles in motion. Initially, before irradiation or start of the degradation, the suspension was air bubbled in the dark for 30 minutes to stabilize the adsorption of dye molecules over the surface of the photocatalyst and to attain an adsorption-desorption equilibrium. Then the photocatalytic degradation was initiated by continuous stirring of the batches of dye treated with NPs in the presence of light irradiated by 300W tungsten

lamp UV lamp (λ > 365 nm) for a period of 3h. To determine the rate of dye decolorization, 3 mL aliquot of dye solution was withdrawn for every 30 min, centrifuged and the absorbance of the supernatant dye solution was measured at 664 nm using UV-Vis spectrophotometer. All the experiments were done at neutral pH and room temperature.

Determination of the mechanism of photocatalytic degradation:

In order to detect the active species generated in the photocatalytic process, which are responsible for the degradation of dye, different radical quenching tests were carried out. Iso-propyl alcohol (i-PrOH), ammonium oxalate (AO) and benzoquinone (BQ) which are commonly used to quench the hydroxyl (•OH), holes and superoxide ($O_2^{\bullet-}$) radicals are added separately at 2mM concentrations to study their effect on dye degradation

RESULTS AND DISCUSSION

Synthesis and characterization of selenium nanoparticles

SeNPs were successfully synthesized using an agrowaste based yeast fermented broth,[29] as reducing agent. The nanoparticle synthesis was identified preliminarily by observing the change in color of the reaction medium, before and after incubation. SeNPs synthesis was evident from gradual change in color of reaction medium from pale yellow to reddish brown (Figure 1) due to the excitation of surface plasmon vibrations in aqueous solution.[33] NPs were formed within 6h of incubation and the rate of synthesis had gradually increased up to 12h as noted by observing visually and through UV-Visible spectral analysis. However, the control sodium selenite (2mM) solution and fermented broth remained unchanged. Depending on their size and shape, colloidal solutions of NPs show difference in intensity of color, due to surface plasmon resonance.[37]

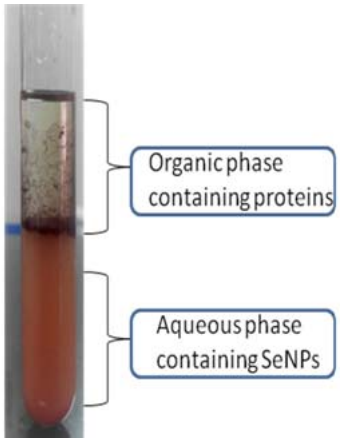

Figure 2 Aqueous two-phase extraction of SeNPs

The green synthesized SeNPs were successfully purified using n-hexanol–water partitioning system (Figure 2). On vortexing the reaction medium, after addition of n-hexanol, SeNPs got settled at the bottom, leaving proteins and other contaminants at the interface of aqueous and organic layers. The SeNPs were primarily characterized by UV–Vis spectroscopy by performing a wavelength scan from 200-750nm, which proved to be a very useful technique for analysis of nanoparticles.[36] The reaction mixture exhibited a maximum absorbance at 540 nm and its intensity increased steadily as a function of reaction time upto 12 h, and beyond which no noticeable increase was observed. Scanning electron microscopy of synthesized SeNPs exhibited a large quantity of dispersive rod shaped nanoparticles with average size of about 170-240 nm, arranged as "flower- like" aggregates (Figure 3b).

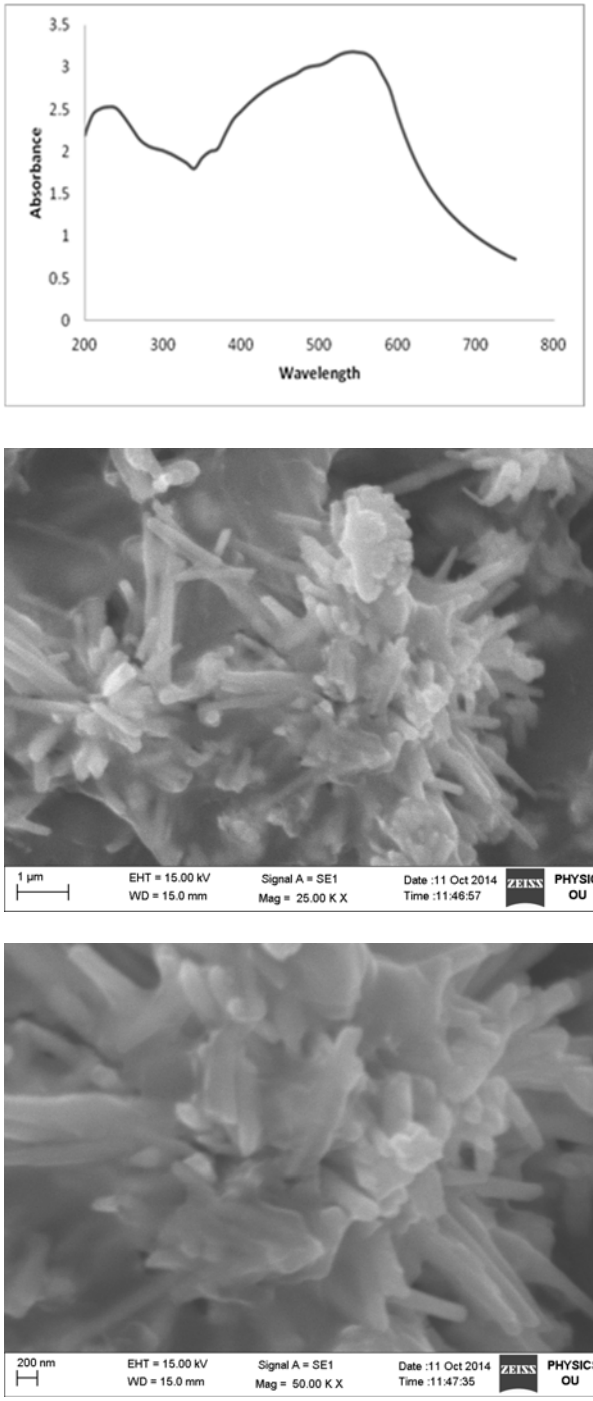

Figure 3 Characterization of SeNps (a) UV – Visible Spectrum (b) Scanning electron microscopic photographs of SeNps at 25 KX and 50 KX magnifications

Element	Weight %	Atomic %
C K	10.79	37.75
N K	4.81	14.43
O K	1.32	3.46
P K	0.14	0.19
S K	0.04	0.05
Se L	82.91	44.13
Totals	100.00	

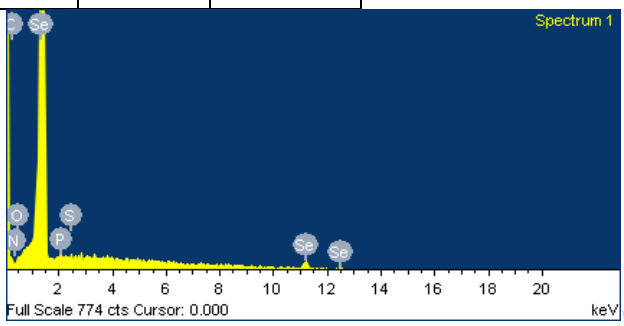

(c)

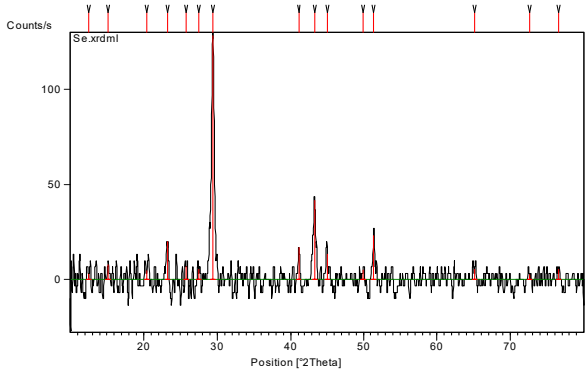

(d)

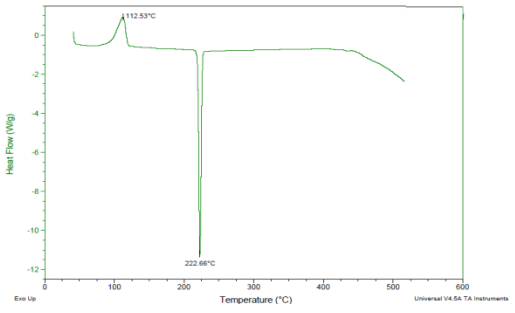

(e)

Figure 3 Characterization of SeNps (c) Energy dispersive spectroscopy of SeNPs (d) X-Ray diffraction pattern (e) Thermogravimetry – Differential scanning calorimetry of SeNPs.

The composition and crystalline structure of the synthesized SeNPs were investigated by EDX and XRD respectively. EDX profile (Figure 3c) showed strong signals for selenium along with weak carbon, oxygen, nitrogen, phosphorus and sulphur peaks. The EDX analysis confirms that selenium is the major component and other elemental signals recorded were might be due to elements from phytochemicals or proteins present in fermented broth. The selenium nano crystallites displayed optical absorption bands with peaks at 1.5, 11.2, and 12.5 keV, which is typical of metallic selenium nano crystallites.[34] The crystalline structure of SeNPs was determined by X-ray diffraction studies as shown in Fig.3d. The diffraction peaks present at 2θ (degrees) of 23.22^0, 29.4^0, 41.15^0, 43.32^0, 45.05^0 and 51.4^0 corresponds to (100), (101), (110), (102), (111) and (201) planes of selenium. The sharpening of peaks clearly indicates that the particles are in nanoregime and diffraction peaks in the 2θ range corresponds to the hexagonal structure of SeNPs and are in good agreement with the standard JCPDS data (JCPDS card No. 06-362). DSC thermogram of the SeNPs, recorded up to 600°C, is shown in Figure 3e. It shows an exothermic transition at 112°C, in addition to the endothermic melting peak at 222.66^0C, which was in account with earlier reports for SeNPs.[37]

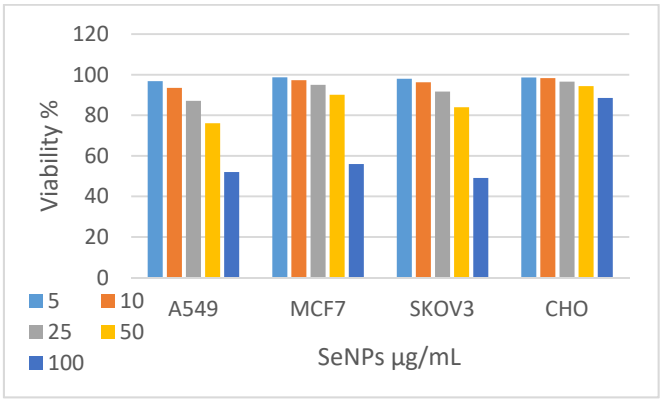

Figure 5 Anticancer activity of SeNPs

Antibacterial activity

Antibacterial activity of SeNPs was tested against different gram positive and gram negative bacteria by standard broth microdilution method. SeNPs showed complete inhibition of *S. aureus* at a concentration of 250µg/mL, whereas no significant inhibition of growth was observed for the other test organisms.

Anticancer activity

Though there are number of reports on the applications of SeNPs in biomedical domain, such observations lack information on their cytocompatibility. Therefore we wanted to assess the green-synthesized SeNPs for their cytocompatibility on normal (non-cancerous) cells and anti-proliferative action on cancerous cells. MTT assay was used to quantitatively evaluate the Cell viability. As shown in Fig. 5, SeNP exhibited a concentration dependent reduction in percentage viability of SKOV3, MCF7, A549 and CHO cells. In comparison, 100µg/mL of SeNP exhibited an intense cytotoxicity against SKOV3, MCF7, A549 cells and very less cytotoxicity against normal cells (Figure 5). Thus, these results suggest that there exists a direct correlation between dose and toxicity of the nanoparticles. Differential interactions of SeNPs with normal cell line and cancerous cell lines need further delving. This may be partially attributed to differential expression and distribution of membrane receptors; membrane potential and the signaling cascades of the corresponding cell lines.

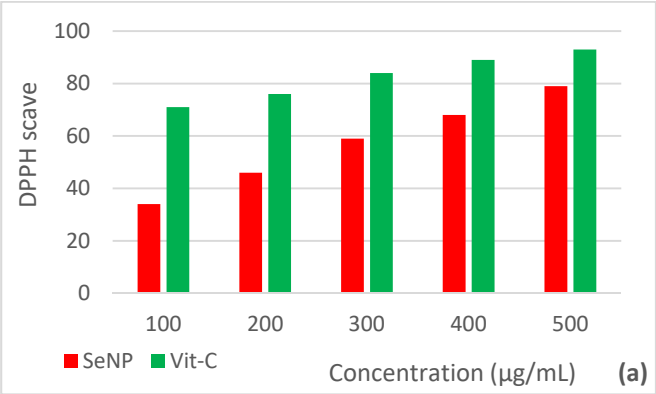

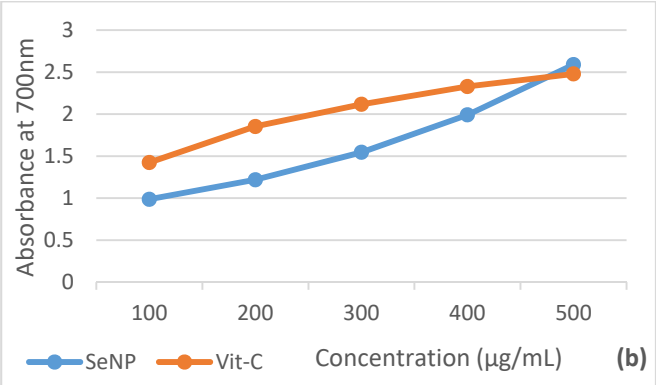

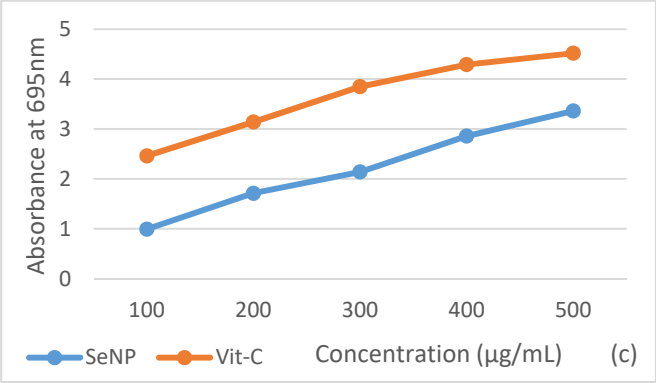

Figure 6 Antioxidant activity of SeNPs (a) DPPH scavenging activity (b) Ferric reducing antioxidant power assay (c) Total antioxidant activity by phosphomolybdenum method

In vitro antioxidant activity

To measure the antioxidant properties of green synthesized SeNPs different antioxidant activity assays, like free radical scavenging activity, ferric reducing antioxidant power (FRAP) and total antioxidant activity by phosphomolybdenum method were performed. Free radical scavenging activity of the SeNPs was assessed by DPPH assay. Free radical scavenging activity of the SeNPs on DPPH radical was found to increase with increase in concentration, showing a maximum of 79% at 500 µg/ml. The standard ascorbic acid, however, at this concentration exhibited 93% inhibition. The IC50 value was found to be 236 µg/mL (Figure 6a).

Figure 6b shows the dose-response bar chart for the reducing powers of the SeNPs. Reducing powers of the SeNPs were found to increase with increasing concentrations. The trend for the ferric ion reducing activities of SeNPs did not differ distinctly from their DPPH free radical scavenging activities (Figure 6a and 6b). Surprisingly, the SeNPs exhibited comparatively better reducing power than ascorbic acid (vitamin C).

The phosphomolybdate method has been routinely used to evaluate the antioxidant capacity. Reduction of Mo (VI) to Mo (V) and subsequent formation of a green phosphate/Mo (V) complex at acidic pH is taken as an index of total antioxidant capacity. As shown in Fig. 6c the SeNPs showed good antioxidant activity but was lesser than standard antioxidants.

Photocatalytic degradation of methylene blue:

In the present study, photocatalytic activity of SeNPs has been investigated by studying the photodegradation of methylene blue (MB) as a function of time. Methylene blue in aqueous solutions has an absorption maxima at 664 nm corresponding to its n-π* transition. The relative absorbance of MB at 664 nm is plotted as a function of time to evaluate the photodegradation rate (Fig.7). Degradation of MB was visualized by decrease in peak intensity within 3 h of irradiation. However, in control sample without exposure to SeNPs, no considerable shift in peak position for MB solution was observed.

It is well documented that the band gap (Eg) of a semiconductor and the generation of the photoinduced e−/h+ pairs are the vital parameters governing the photocatalytic behavior of semiconductors.[38] In general, the principle mechanism of photocatalysis is as follows: When light (hυ ≥ Band gap) strikes the photocatalyst, it absorbs some energy leading to the excitation of electrons from the valence band (vb) to the conduction band (cb) of photocatalyst, generating a positively charged hole in the valence band (h_{vb}^+) and negative charge in the conduction band (e_{cb}^-) according to the following equation:

$$SeNP + h\upsilon \rightarrow h_{vb}^+ + e_{cb}^- \quad (1)$$

The so formed conduction band electrons and the valence band holes then migrate to the surface of photocatalyst where they react with the chemisorbed O_2 and/or H_2O molecules to form reactive oxygen species such as $O_2^{\bullet-}$, $OH^\bullet$ radicals etc. These hyperactive radicals (e.g., •OH, $O_2^{\bullet-}$) and/or photogenerated holes which are considered as capable of directly oxidizing many organic pollutants, attack dye molecules successively to break down into smaller fragments that finally decompose into simple inorganic minerals.

$$O_2 + e_{cb}^- \rightarrow O_2^{\bullet-} \quad (2)$$

$$H_2O + h_{vb}^+ \rightarrow OH^\bullet + H^+ \quad (3)$$

$$O_2^{\bullet-} + H^+ \rightarrow HO_2^\bullet \quad (4)$$

$$2HO_2^\bullet \rightarrow H_2O_2 + O_2 \quad (5)$$

$$H_2O_2 \rightarrow 2\ OH^\bullet \quad (6)$$

$$O_2^{\bullet-} / OH^\bullet / h_{vb}^+ + \text{MB dye} \rightarrow \text{Byproducts} \quad (7)$$

Scheme 1. Possible degradation mechanism of methylene blue dye by the SeNPs

In order to detect the active species generated in the photocatalytic process, which are responsible for the

degradation of MB dye solution, different radical quenching tests were carried out. Iso-propyl alcohol (i-PrOH), ammonium oxalate (AO) and benzoquinone (BQ) which are commonly used to scavenge the hydroxyl (•OH), holes and superoxide ($O_2^{\bullet-}$) radicals respectively[38] are added to the photocatalytic reaction mixture and observed for their effect on dye degradation. As shown in Fig. 8, compared with no scavenger, the addition of BQ distinctly inhibited the degradation of dye, whereas i-PrOH and AO decreased the degradation rate slightly. Based on above results, it is reckoned that superoxide ($O_2^{\bullet-}$) radicals played the pivotal role whereas hydroxyl (•OH) radicals and holes (h+) play minor role in the photocatalytic degradation of MB dye. Based on the above observations, the possible photocatalytic degradation mechanism was deduced in scheme.1 and also shown in Figure 9.

CONCLUSION

SeNPs were made by green synthesis using an agrowaste based yeast fermented broth as reducing agent. The green synthesized SeNPs were characterized and evaluated for their antibacterial, anticancer, antioxidant and photocatalytic efficiency. The green synthesized SeNPs were found to exhibit good biological activities. The nanoparticles were found to be active in degrading methylene blue solution with visible light illumination. This may pave way for their application in water purification systems and environmental bioremediation.

ACKNOWLEDGEMENT

The authors gratefully acknowledge financial support by UGC under UPE project for financial support to carry out this work and fellowship to GGK.

REFERENCES

1. K.M.M. Abou El-Nour, A.a. Eftaiha, A. Al-Warthan, R.A.A. Ammar. Synthesis and applications of silver nanoparticles. *Arabian Journal of Chemistry*, **2010**, 3(3), 135-140.
2. K.B. Narayanan, N. Sakthivel. Biological synthesis of metal nanoparticles by microbes. *Advances in colloid and interface science*, **2010**, 156(1), 1-13.
3. L. Rastogi, J. Arunachalam. Sunlight based irradiation strategy for rapid green synthesis of highly stable silver nanoparticles using aqueous garlic (Allium sativum) extract and their antibacterial potential. *Materials Chemistry and Physics*, **2011**, 129(1–2), 558-563.
4. P.P. Gan, S.H. Ng, Y. Huang, S.F.Y. Li. Green synthesis of gold nanoparticles using palm oil mill effluent (POME): A low-cost and eco-friendly viable approach. *Bioresource technology*, **2012**, 113, 132-135.
5. X. Wei, M. Luo, W. Li, L. Yang, X. Liang, L. Xu, P. Kong., H. Liu, Synthesis of silver nanoparticles by solar irradiation of cell-free Bacillus amyloliquefaciens extracts and AgNO3. *Bioresource Technology*, **2012**, 103(1), 273-278.
6. J. Singh, S. Kumar, B. Rathi, K. Bhrara, B.S. Chhikara. Therapeutic analysis of Terminalia arjuna plant extracts in combinations with different metal nanoparticles. *J. Mat. NanoSci.*, **2015**, 2(1), 1-7.
7. T. Bhuyan,, K. Mishra, M. Khanuja, R. Prasad, A. Varma. Biosynthesis of zinc oxide nanoparticles from Azadirachta indica for antibacterial and photocatalytic applications. *Materials Science in Semiconductor Processing*, **2015**, 32, 55-61.
8. J.K. Yan, J.-L. Liu,, Y.-J. Sun,, S. Tang, Z.-Y. Mo, Y.-S. Liu. Green synthesis of biocompatible carboxylic curdlan-capped gold nanoparticles and its interaction with protein. *Carbohydrate Polymers*, **2015**, 117, 771-777.
9. I.M. Banat, P. Nigam, D. Singh, R. Marchant. Microbial decolorization of textile-dyecontaining effluents: A review. *Bioresource Technology*, **1996**, 58(3), 217-227.
10. C. O'Neill, F.R. Hawkes, D.L. Hawkes, N.D. Lourenço, H.M. Pinheiro, W. Delée. Colour in textile effluents – sources, measurement, discharge consents and simulation: a review. *Journal of Chemical Technology & Biotechnology*, **1999**, 74(11), 1009-1018.
11. H. Sudrajat, S. Babel, H. Sakai, S. Takizawa. Rapid enhanced photocatalytic degradation of dyes using novel N-doped ZrO2. *Journal of Environmental Management*, **2016**, 165, 224-234.
12. R. Maas, S. Chaudhari. Adsorption and biological decolourization of azo dye Reactive Red 2 in semicontinuous anaerobic reactors. *Process Biochemistry*, **2005**, 40(2), 699-705.
13. M. Chander, D.S.. Arora. Evaluation of some white-rot fungi for their potential to decolourise industrial dyes. *Dyes and Pigments*, **2007**, 72(2), 192-198.
14. V.K. Gupta, R. Jain, A. Mittal, M. Mathur, S. Sikarwar. Photochemical degradation of the hazardous dye Safranin-T using TiO2 catalyst. *Journal of Colloid and Interface Science*, **2007**, 309(2), 464-469.
15. R. Jain, S. Sikarwar. Removal of hazardous dye congored from waste material. *Journal of Hazardous Materials*, **2008**, 152(3), 942-948.
16. S.M. Ghoreishi, R. Haghighi. Chemical catalytic reaction and biological oxidation for treatment of non-biodegradable textile effluent. *Chemical Engineering Journal*, **2003**, 95(1–3), 163-169.
17. D.K. Tiwari, J. Behari, P. Sen. Application of Nanoparticles in Waste Water Treatment 1, **2008**.
18. Z. Zhang, W. Wang, W. Yin, M. Shang, L. Wang, S. Sun. Inducing photocatalysis by visible light beyond the absorption edge: Effect of upconversion agent on the photocatalytic activity of Bi2WO6. *Applied Catalysis B: Environmental*, **2010**, 101(1–2), 68-73.
19. S.S. Thind, G. Wu, A. Chen. Synthesis of mesoporous nitrogen–tungsten co-doped TiO2 photocatalysts with high visible light activity. *Applied Catalysis B: Environmental*, **2012**, 111–112, 38-45.
20. H. Kisch. Semiconductor Photocatalysis—Mechanistic and Synthetic Aspects. *Angewandte Chemie International Edition*, **2013**, 52(3), 812-847.
21. Y.-C. Cao, Z. Fu, W. Wei, L. Zou, T. Mi, D. He, C. Yan, X. Liu, Y. Zhu, L. Chen, Y. Sun. Reduced graphene oxide supported titanium dioxide nanomaterials for the photocatalysis with long cycling life. *Applied Surface Science*, **2015**, 355, 1289-1294.
22. D. Ljubas, G. Smoljanić, H. Juretić. Degradation of Methyl Orange and Congo Red dyes by using TiO2 nanoparticles activated by the solar and the solar-like radiation. *Journal of Environmental Management*, **2015**, 161, 83-91.
23. M. Stoller, J.M.O. Pulido, L. Di Palma, A.M. Ferez. Membrane process enhancement of 2-phase and 3-phase olive mill wastewater treatment plants by photocatalysis with magnetic-core titanium dioxide nanoparticles. *Journal of Industrial and Engineering Chemistry*, **2015**, 30, 147-152.
24. S. Sardar, P. Kar, S.K. Pal. The Impact of Central Metal Ions in Porphyrin Functionalized ZnO/TiO2 for Enhanced Solar Energy Conversion. *Journal of Materials NanoScience*, **2014**, 1(1), 12-30.
25. W. Yu, X. Liu, L. Pan, J. Li, J. Liu, J. Zhang, P. Li, C. Chen, Z. Sun. Enhanced visible light photocatalytic degradation of methylene blue by F-doped TiO2. *Applied Surface Science*, **2014**, 319, 107-112.
26. V.V. Poborchii, A.V. Kolobov, K. Tanaka. An in situ Raman study of polarization-dependent photocrystallization in amorphous selenium films. *Applied physics letters*, **1998**,72, 1167.
27. E.A. Martino, D. Winterton, P. Nardelli, L. Pasin, M.G. Calabrò, T. Bove, G. Fanelli, A. Zangrillo, G. Landoni. The Blue Coma: The Role of Methylene Blue in Unexplained Coma After Cardiac Surgery. *Journal of Cardiothoracic and Vascular Anesthesia*, **2016**, 30(2), 423-427.
28. Z. Chen, J. Zhang, J. Fu, M. Wang, X. Wang, R. Han, Q. Xu. Adsorption of methylene blue onto poly(cyclotriphosphazene-co-4,4′-sulfonyldiphenol) nanotubes: Kinetics, isotherm and thermodynamics analysis. *Journal of Hazardous Materials*, **2014**, 273, 263-271.

29. K. Gnaneshwar Goud, K. Chaitanya, G. Reddy. Enhanced production of β-d-fructofuranosidase by Saccharomyces cerevisiae using agro-industrial wastes as substrates. *Biocatalysis and Agricultural Biotechnology*, **2013**, 2(4), 385-392.
30. K. Shimada, K. Fujikawa, K. Yahara, T. Nakamura. Antioxidative properties of xanthan on the autoxidation of soybean oil in cyclodextrin emulsion. *Journal of agricultural and food chemistry*, **1992**, 40(6), 945-948.
31. S.B. Zhang, Z. Wang, S.Y. Xu. Antioxidant and antithrombotic activities of rapeseed peptides. *Journal of the American Oil Chemists' Society*, **2008**, 85(6), 521-527.
32. P. Prieto, M. Pineda, M. Aguilar. Spectrophotometric quantitation of antioxidant capacity through the formation of a phosphomolybdenum complex: specific application to the determination of vitamin E. *Analytical biochemistry*, **1999**, 269(2), 337-341.
33. S. Dwivedi, A.A. Khedhairy, M. Ahamed, J. Musarrat. Biomimetic synthesis of selenium nanospheres by bacterial strain JS-11 and its role as a biosensor for nanotoxicity assessment: a novel Se-bioassay. *PloS one*, **2013**, 8(3), e57404.
34. R.S. Oremland, M.J. Herbel, J.S. Blum, S., Langley, T.J. Beveridge, P.M.. Ajayan, T. Sutto, A.V. Ellis, S. Curran. Structural and spectral features of selenium nanospheres produced by Se-respiring bacteria. *Applied and environmental microbiology*, **2004**, 70(1), 52-60.
35. P. Sonkusre, R. Nanduri, P. Gupta, S.S. Cameotra. Improved extraction of intracellular biogenic selenium nanoparticles and their specificity for cancer chemoprevention. *J Nanomed Nanotechnol*, **2014**, 5(194), 2.
36. A.N. Wang, Y. Teng, X.-f. Hu, L.-h. Wu, Y.-j. Huang, Y.-m. Luo, P. Christie. Diphenylarsinic acid contaminated soil remediation by titanium dioxide (P25) photocatalysis: Degradation pathway, optimization of operating parameters and effects of soil properties. *Sci. Total Environ.*, **2016**, 541, 348-355.
37. C.P. Shah, M. Kumar, K.K. Pushpa, P.N. Bajaj. Acrylonitrile-induced synthesis of polyvinyl alcohol-stabilized selenium nanoparticles. *Crystal Growth and Design*, **2008**, 8: 4159-4164.
38. N.K. Veldurthi, S. Palla, R. Velchuri, P. Guduru, V. Muga. Degradation of mixed dyes in aqueous wastewater using a novel visible light driven LiMgO. 5MnO. $5O_2$ photocatalyst. *Materials Express*, **2015**, 5, 445-450.